J Appl Electrochem (2012) 42:427–434
DOI 10.1007/s10800-012-0416-2

ORIGINAL PAPER

Gold nanoparticle–polypyrrole composite modified TiO_2 nanotube array electrode for the amperometric sensing of ascorbic acid

T. G. Satheesh Babu · Dhanya Varadarajan · Gayathri Murugan · T. Ramachandran · Bipin G. Nair

Received: 15 January 2012 / Accepted: 12 April 2012 / Published online: 27 April 2012

Abstract Titanium dioxide (TiO_2) nanotubes were fabricated by anodisation of titanium foil in 0.15 M ammonium fluoride in an aqueous solution of glycerol (90 % v/v). Electropolymerisation of pyrrole and deposition of gold nanoparticles on to the TiO_2 nanotube array electrode were carried out by cyclic voltammetry (CV). Electrochemical characterization of the sensor was performed by CV and electrochemical impedance spectroscopy. The morphology of the electrode was studied after every step of modification using field emission scanning electron microscope and atomic force microscope. The sensor was tested for AA and other biomolecules in phosphate buffered saline solution of pH 7 using CV, differential pulse voltammetry and amperometry. The sensor exhibited very high sensitivity of 63.912 μA mM^{-1} cm^{-2} and excellent selectivity to ascorbic acid (AA) in the presence of other biomolecules such as uric acid, dopamine, glucose and para-acetaminophen. It also showed very good linearity ($R = 0.9995$) over a wide range (1 μM–5 mM) of detection. The sensor was tested for AA in lemon and found its concentration to be 339 mg ml^{-1}.

Keywords Titanium dioxide nanotube arrays · Gold nanoparticles · Polypyrrole · Ascorbic acid sensor

1 Introduction

Last decade has witnessed the preparation, characterization and application of various nanostructures like nanoparticles, nanotubes, nanowires and nanorods due to their special properties. Among the 1-D architectures, nanotube arrays have a higher surface area than nanowires due to the additional surface area enclosed inside the hollow structure [1]. TiO_2 nanotube, one of the recent additions in this group of materials, is an oxide semiconducting material which is explored extensively for various applications including gas sensor [2–9], dye sensitized solar cell [10–15] and biosensor [16–19]. TiO_2 nanotubes can be easily fabricated by electrochemical anodisation from fluoride electrolytes [20].

Although different nanomaterials were employed for the fabrication of electrochemical sensors and biosensors for the quantitative determination of AA, the use of gold nanoparticles attracted the attention of several researchers due to their unique properties such as good conductivity, useful electrocatalytic behaviour and biocompatibility [21–26]. It is believed that the catalytic activity of AuNPs originates from the quantum scale dimension and is attributed to the large surface-to-volume ratio and the existence of special binding sites on their surface [27]. Several strategies were employed to immobilize AuNPs on the electrode substrate which includes electrodeposition [28] and immobilization through covalent or electrostatic interactions with the self-assembled monolayers terminated

Electronic supplementary material The online version of this article (doi:10.1007/s10800-012-0416-2) contains supplementary material, which is available to authorized users.

T. G. Satheesh Babu (✉) · T. Ramachandran
Department of Sciences, Amrita School of Engineering, Amrita Vishwa Vidyapeetham, Ettimadai P. O., Coimbatore 641105, India
e-mail: tgsatheesh@gmail.com

D. Varadarajan · G. Murugan
Department of Polymer Engineering, Amrita School of Engineering, Amrita Vishwa Vidyapeetham, Ettimadai P. O., Coimbatore 641105, India

B. G. Nair
Amrita School of Biotechnology, Amrita Vishwa Vidyapeetham, Amritapuri, Clappana P. O., Kollam 690525, India

with suitable functional groups [22, 29–31]. Individual and simultaneous determination of nanomolar UA and AA using enlarged, citrate-stabilized AuNPs self-assembled 2,5-dimercapto-1,3,4-thiadiazole monolayer modified Au electrode was studied by amperometric method [32]. AA in the presence of DA was determined at multiwalled carbon nanotube–silica network–gold nanoparticles based nanohybrid modified electrode using DPV [33].

The catalytic efficiency and hence the current response of the amperometric sensor are always highly related to the electrode surface area. Various methods were used to increase the electrode surface area, such as the modification of electrodes with carbon nanofibers [34, 35], carbon nanotubes [36–38] and using nanoporous electrodes [39, 40]. In recent years, TiO_2 nanotube arrays have drawn interest of several researchers due to the ease of preparation, high orientation, large surface area, high uniformity, and excellent biocompatibility [41–45]. A Co–Ag–Pt nanoparticle-decorated TiO_2 nanotube array was found to show a nine fold increase in catalytic activity when compared to platinum electrode [42]. Recently, TiO_2 nanotube based glucose biosensors of good selectivity and sensitivity were made using horse radish peroxidase [45] and glucose oxidase [46]. AuNP modified TiO_2 nanotube array biosensors were adopted for the determination of hydrogen peroxide [16] and Pt–Au nanoparticles modified TiO_2 nanotube array electrodes were used for the immobilisation of glucose oxidase and used for the amperometric detection of glucose [47]. Very recently, Wang et al. [48] reported the use of TiO_2 nanotube array-Ni composite electrodes for non-enzymatic amperometric detection of glucose. AuNPs were electrodeposited on TiO_2 nanotube arrays and used for the quantitative determination of AA [49]

It is well known that conducting polymers (CPs) have electrocatalytic activities towards various substrates, including ions and organic compounds [50]. Among all CPs, polypyrrole (PPy) finds extensive application in the development of biosensors, because it has moderate electrical conductivity and can be synthesized electrochemically under biocompatible conditions [51, 52]. CPs are often considered to be useful matrices for the immobilization of the dispersed noble metal catalysts. Because of a relatively high electric conductivity of CPs, it is possible to shuttle the electrons through polymer chains between the electrode and dispersed metal particles, where the electrocatalytic reaction occurs. Thus, an efficient electrocatalysis can be achieved on the surface of these composite materials. Recent trend is towards the development of metal nanoparticles-PPy composites for biosensor applications [53–55]. Biosensor for the determination of epinephrine and uric acid in the presence of AA was fabricated by electrochemical deposition of gold nanoclusters on ultrathin overoxidized PPy film [53]. A micro-potentiometric haemoglobin immunosensor based on electrochemically synthesized PPy–AuNP composite modified electrode was reported [54]. Biosensor for organophosphate pesticides was developed using AuNP–PPy nanowires composite film and immobilized acetylcholinesterase on glassy carbon electrode [55].

In the present study, a highly sensitive and selective sensor for the detection of ascorbic acid was developed by the electropolymerisation of pyrrole on TiO_2 nanotube arrays followed by the electrodeposition of AuNPs. The sensor was characterized for its morphological and electrochemical characteristics and tested with AA and other biomolecules and very promising results were obtained. Sensor was also used for the testing of ascorbic acid in lemon juice.

2 Experimental

2.1 Chemicals and reagents

Titanium foil of (99.7 %) 0.25 mm thickness, pyrrole (98 %) and glucose (99.9 %) were purchased from Sigma-Aldrich and used as received. L-ascorbic acid (99 %) and uric acid (99 %) were procured from Lobachemie, India. Ammonium fluoride, glycerol, chloroauric acid and other chemicals were of analytical grade and used without further purification. 5 mM potassium ferricyanide in 1 M KCl was used for electrochemical characterisation and 0.1 M PBS of pH 7 for amperometric measurements. Solutions used in this study were prepared with double distilled water.

2.2 Instrumentation

Anodization of titanium foil was carried out using a conventional electrolytic cell with titanium foil as the anode and platinum foil as the cathode. An indigenously fabricated DC power supply (5 A, continuous variable 60 V) was employed for anodisation and a magnetic stirrer for agitation of the electrolyte during anodization. The morphology of the anodized titanium foil was studied by a variable pressure FESEM (Hittachi SU 6600) and AFM (NT-MDT NTEGRA Prima). All electrochemical experiments were carried out using CHI 660C electrochemical workstation (CH Instruments, Austin, TX, USA), with a conventional three-electrode cell consisting of TiO_2 or modified TiO_2 as working, platinum foil as counter and silver/silver chloride (Ag/AgCl) as reference electrode. All potentials measured in this study were referenced to Ag/AgCl (3 M KCl) electrode.

2.3 Fabrication of TiO_2

Prior to anodization, the titanium strips were washed with double distilled water, followed by ethyl alcohol and acetone and then dried in nitrogen atmosphere. Titanium was

potentiostatically anodized from a mixture of glycerol and water (10 %v/v) containing ammonium fluoride (0.15 M) at 20 V for 5 h [56]. The anodized specimen was washed in double distilled water and preserved in deaerated double distilled water.

2.4 Fabrication of sensor electrodes

The electrodeposition of PPy on TiO_2 nanotube electrode was carried out by immersing in a solution of 0.1 M pyrrole in 1 M KCl and cycled five times between 0 and 1.2 V at a scan rate of 100 mV s^{-1} and rinsed with water. It was denoted as PPy/TiO_2. Electrodeposition of AuNPs on this was carried out by CV in a potential window of 0.5 to −1.0 V at a scan rate of 100 mV s^{-1} from 5 mM solution of chloroauric acid. Then, the modified electrode was taken out and rinsed with water. It is denoted as AuNP/PPy/TiO_2.

2.5 Electrochemical characterisation

All electrochemical characterization was carried out in 5 mM potassium ferricyanide in 1 M potassium chloride. CVs were carried out in a potential range of 0–0.6 V at a scan rate of 100 mV s^{-1}. EIS of the bare and modified electrodes was carried out at open circuit potentials, in the frequency range of 0.01 Hz–100 kHz with potential amplitude of 10 mV. The impedance spectra were plotted in the form of complex plane diagrams.

2.6 Electrochemical oxidation of AA

The CV and linear sweep voltammetry (LSV) were carried out in 0.1 M PBS in a potential window of 0–0.6 V at a scan rate of 100 mV s^{-1}. DPV experiments were conducted at a scan rate of 20 mV s^{-1} under 50 mV pulse amplitude, pulse width of 50 ms and pulse time of 200 ms. The steady state response of the sensor to AA was carried out at 0.2 V in a constantly stirred solution of 0.1 M PBS. 10 µl of AA solution was injected at regular intervals so that the resultant concentration varied from 1 µM to 5 mM. The interference of other biomolecules was studied by injecting 10 µl of the solution into the test solution. All experiments were conducted at room temperature (25 ± 2 °C) and were repeated at least three times to check reproducibility.

3 Results and discussion

3.1 Surface characterization

Figure 1 shows a comparison of the morphology of the bare TiO_2, PPy/TiO_2 and AuNP/PPy/TiO_2 electrodes by FESEM and AFM.

Highly ordered titanium dioxide arrays can be seen in Fig. 1a. The diameter of the nanotube is about 40 nm. From the side view of the nanotube arrays (Fig. 1b), the length of the tube was found to be about 1.58 µm. Figure 1c is PPy coated (for five potential cycles) on TiO_2 electrodes. It is seen from the image that the coating of the PPy is not uniform. This arises because the anodized surface is not planar in the nanoscopic regime and hence the electric field on the surface is not uniformly distributed resulting in the formation of polymer at more projected areas. It was found that AuNPs deposited on the sites, where PPy has formed (Fig. 1d) again due to the differential electric field. Here, the deposition of AuNPs was carried out for four potential cycles. On increasing the number of potential cycles, the size of the AuNPs increased and formed nanoclusters. Figure 1e shows the FESEM image for ten potential cycles of AuNPs deposition. The AFM study carried out with AuNP/PPy/TiO_2 supports these observations. The particle size of the AuNP deposited by four potential cycles (Fig. 1f) was much smaller than the one obtained after eight potential cycles of deposition (Fig. 1g).

Since the PPy has inherent ability to accommodate metal nanoparticles and the nanotubular structures of the TiO_2 makes the modified electrode a suitable matrix for AuNPs and prevent aggregation. After deposition of AuNPs on the PPy/TiO_2 the colour turns to reddish violet which is the typical colour of gold nanoparticle. This was not in the case of direct electrodeposition of gold on unmodified titanium electrode from the same chloroauric acid solution under similar conditions and a golden yellow coloured deposit was obtained. From this observation it is reasonable to assume that the deposition of Au on the modified electrode takes place as gold nanoparticles and on the unmodified electrode as bulk gold.

3.2 Electrochemical characterisation of sensor electrodes

Figure 2a shows the CVs of the bare and modified electrodes in 5 mM potassium ferricyanide solution in 1 M KCl. The curve ‘a’ shows no characteristic peak in ferricyanide solution, indicating that the TiO_2 nanotube electrode surface does not catalyse the redox of ferricyanide. The curve ‘b’ depicts an increase in charging current because of the deposition of PPy on the TiO_2 nanotube electrode which is a characteristic feature of the CPs coated electrodes. The curve ‘c’ obtained on the AuNP/PPy/TiO_2 electrode shows typical redox peaks of $[Fe(CN)_6]^{3-/4-}$. The peak observed was sharp and peak separation was only 80 mV indicating good electronic communication between the AuNPs and titanium through the PPy/TiO_2 matrix.

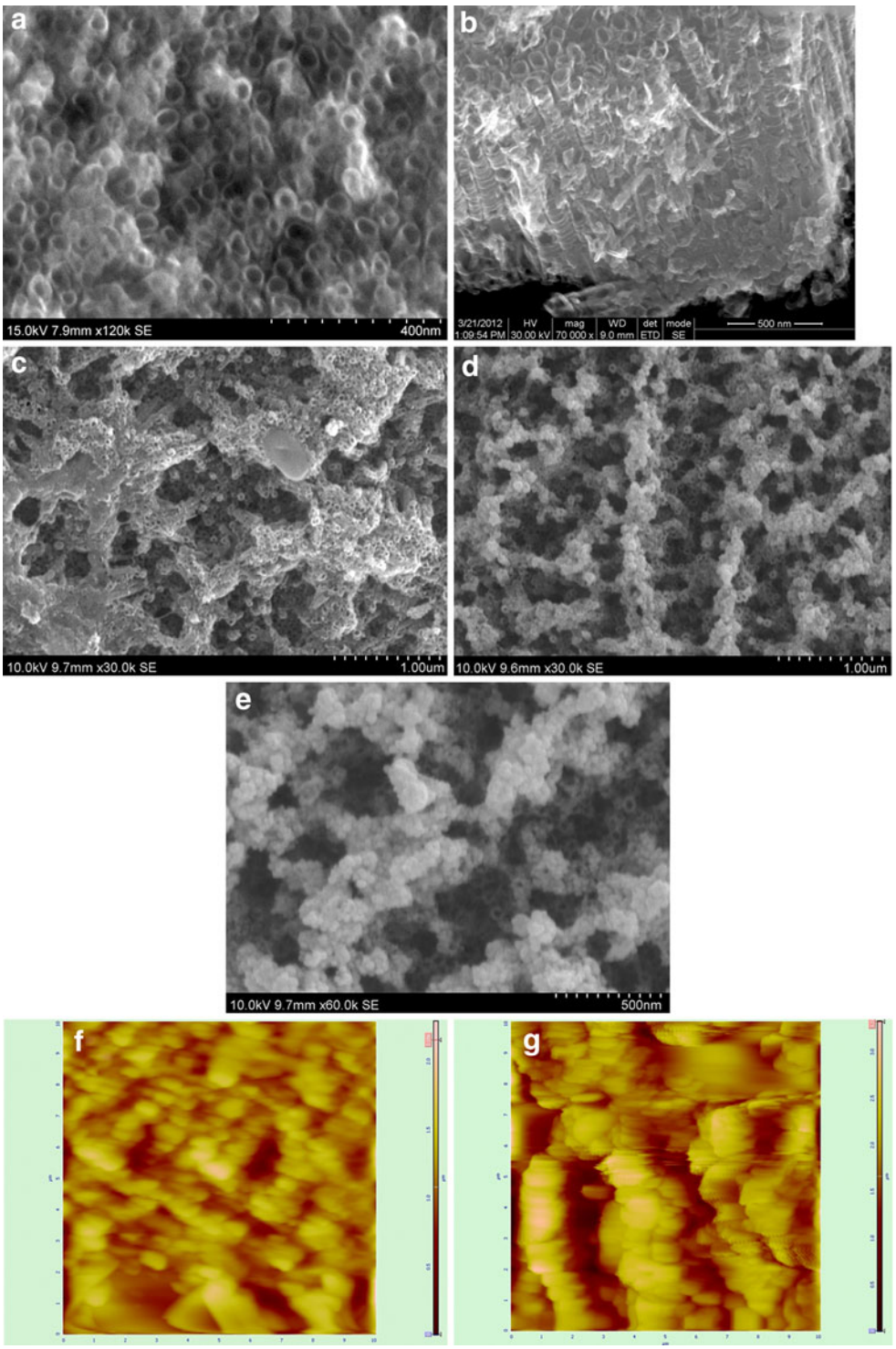

Fig. 1 FESEM images **a** TiO_2 nanotube arrays, **b** side view of the TiO_2 nanotube arrays, **c** PPy/TiO_2, **d** AuNP deposited (for four potential cycles) PPy/TiO_2, **e** AuNP deposited (for ten potential cycles) PPy/TiO_2. **f** and **g** are AFM images of the AuNP/PPy/TiO_2 electrodes, after four and eight potential cycles of AuNP deposition

The effect of AuNPs on the electrocatalyic activity was studied by increasing the deposit of AuNPs on the TiO_2 electrode. The CVs carried out after 2, 4, 6, 8, 10 and 12 cycles of AuNP deposition is presented in Fig. 2b and it shows that the peak current increases with increase in AuNPs on the electrode surface. As reported, the electron transfer reaction of $[Fe(CN)_6]^{3-/4-}$ depends on the surface coverage of AuNPs [30, 57, 58], and hence the observed

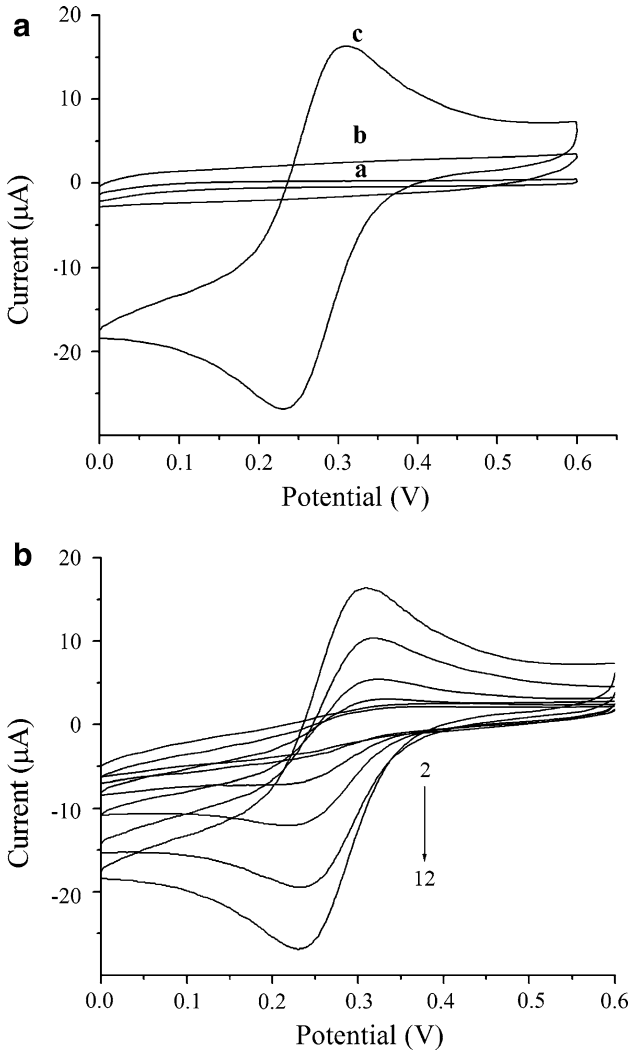

Fig. 2 CVs at 100 mV s^{-1} in 1 mM potassium ferricyanide in 0.1 M KCl on, **a** (*a*) TiO_2 (*b*) PPy/TiO_2 and (*c*) $AuNP/PPy/TiO_2$ electrodes and **b** $AuNP/PPy/TiO_2$ electrodes, 2–12 corresponding to the CV in ferricyanide after two, four, six, eight, ten and 12 potential cycles of AuNP deposition

increase in peak current with the increase in AuNPs. Further, the CVs observed in ferricyanide with repeated immobilization of AuNPs showed same peak separation which indicates that the particles did not aggregate but dispersed, as the size of the immobilized AuNPs increases the peak separation also increases [59]. The low value of peak separation suggests that the electron transfer on the modified electrode is relatively fast [59].

Again, the peak current increases linearly with square root of scan rate (Fig. S1 in the supporting information) with a linear regression equation, i_{pa} (μA) = 2.7232 + 1.1921$v^{1/2}$ (mV s^{-1})$^{1/2}$ and (r = 0.9989). This illustrates that the redox of ferricyanide is a typical diffusion controlled process on the modified electrode.

The electrochemical impedance spectroscopic (EIS) studies of the bare and modified electrodes show that the electron transfer resistance (R_{et}) of the TiO_2 electrode decreases due to the deposition of PPy on the electrode (Fig. S2 in the supporting information). Further, repeated immobilization of AuNPs on the PPy/TiO_2 electrode resulted in a gradual decrease of impedance. This again confirms that during each CV in chloroauric acid the amount of AuNPs deposited on the electrode surface increases.

3.3 Electrocatalytic oxidation of AA

The DPVs of AA oxidation on bare TiO_2, PPy/TiO_2 and $AuNP/PPy/TiO_2$ electrodes are presented in Fig. 3. No characteristic peak on TiO_2 and PPy/TiO_2 (curve *a* and *b*) was obtained indicating no oxidation of AA. But on the PPy/TiO_2 electrode, an increase in charging current was observed due to the coating of CP. On the AuNPs modified electrode a sharp peak at 0.15 V appears corresponding to the oxidation of AA to dehydroascorbic acid. This observed potential is about 0.34 V less positive than that of the oxidation on bare gold electrode [60, 61], illustrating the electrocatalytic effect of the AuNPs on the electrode surface. Since the oxidation takes place at a lower potential, the commonly interfering molecules which got oxidized at a relatively positive potential will not interfere in the detection of AA. Further deposition of AuNPs on the electrode increases the peak current depicting the enhancement of electrocatalytic activity towards the oxidation of AA. A similar trend in peak current for AA oxidation was observed up to 12 CVs of AuNP immobilization. The peak current increases linearly with the concentration of AA with a very slight shift in peak potential

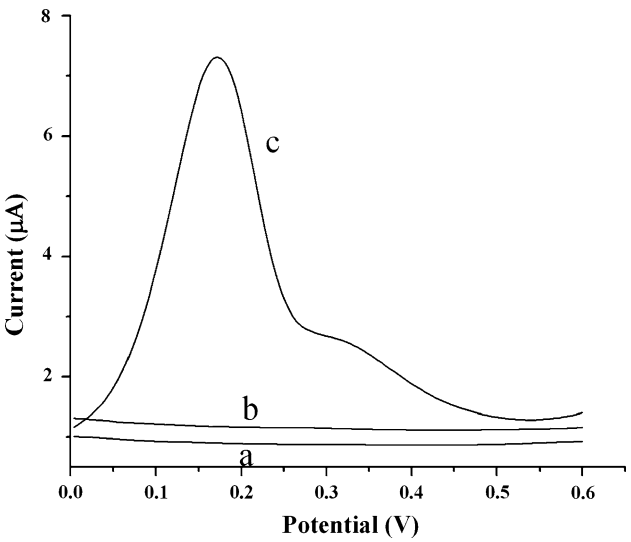

Fig. 3 Differential pulse voltammograms on **a** TiO_2, **b** PPy/TiO_2 and **c** $AuNP/PPy/TiO_2$ electrodes in PBS containing 100 μM AA

(Fig. 4). Each addition corresponds to an increment of 100 μM and a linear response was observed with a linear regression equation $i_p(\mu A) = 0.0083C\ (\mu M) + 1.3041$ ($r = 0.9989$) throughout the concentration.

After 12 potential cycles of AuNP deposition, further depositions did not cause any increase in the peak current for AA oxidation, instead the peak current was found to decrease considerably. Again, a new peak was observed at 0.30 V (Fig. 5). The peak current intensity increases with concentration of AA accompanied with a positive shift in peak potential. The reduction in peak current and appearance of new peak can be attributed to the conversion of AuNPs into the bigger clusters of gold at very high gold loading [62] since the size of the nanocluster and their aggregation state could influence the catalytic efficiency.

CV obtained in 100 μM AA in 0.1 M PBS (Fig. S3 in the supporting information) showed an anodic peak but no peak was observed in the cathodic scan indicating irreversibility of electrocatalytic oxidation of AA on AuNP/PPy/TiO_2 electrode. LSVs obtained at various scan rates showed that the peak current varies linearly with square root of the scan rate, which establishes the diffusion controlled nature of the oxidation process (Fig. S4 in the supporting information).

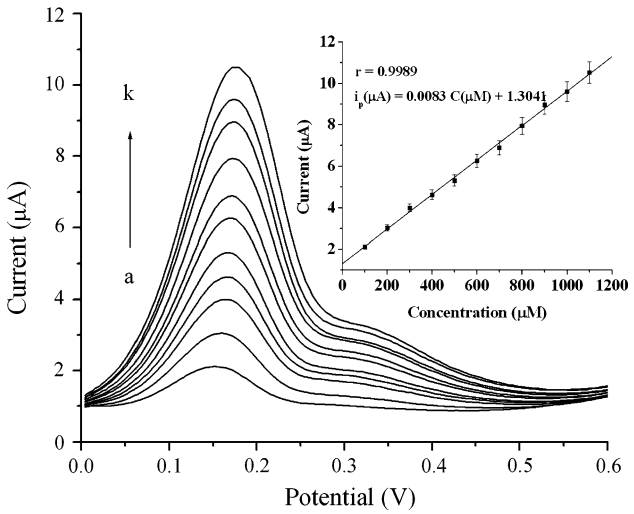

Fig. 4 Differential pulse voltammograms on AuNP/PPy/TiO_2 electrodes in 0.1 M PBS. Each addition of AA increased the concentration by 100 μM (**a**–**k**). *Inset* shows the corresponding calibration plot

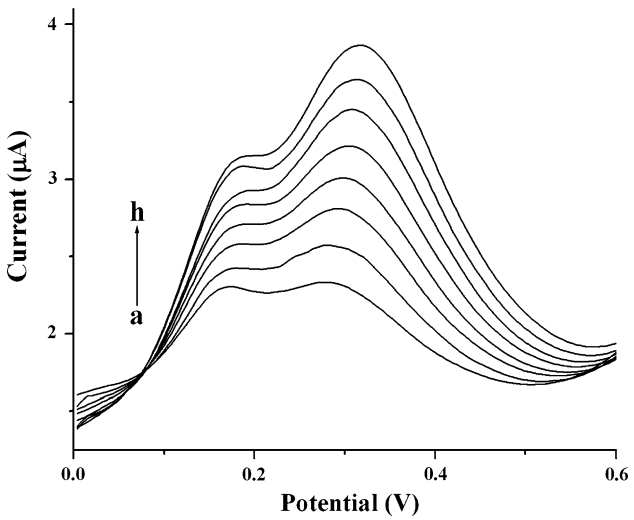

Fig. 5 Differential pulse voltammograms on AuNP/PPy/TiO_2 electrode (after 14 potential cycles of AuNP deposition) in 0.1 M PBS. Each addition of AA increased the concentration by 100 μM (**a**–**h**)

3.4 Amperometric detection of AA

The steady state current response observed at 0.2 V with successive additions of AA is shown in Fig. 6a. Time required to obtain a stable response after the injection of

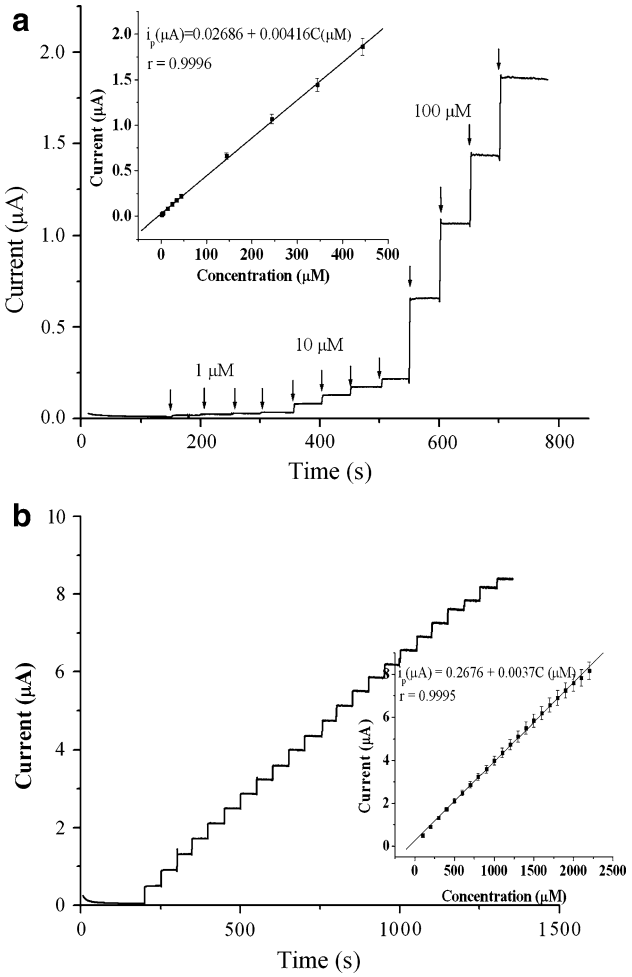

Fig. 6 The steady state current response of the AuNP/PPy/TiO_2 electrode to AA in a constantly stirred solution of 0.1 M PBS at 0.2 V **a** by successive additions of various concentrations of AA (*inset* the calibration curve) and **b** by successive additions of 100 μM of AA (*inset* shows the calibration curve)

AA was <1 s. Three different ranges of concentrations were tested by successive additions of AA in 0.1 M PBS of pH 7. The first set of four additions was introduced in increments of 1 μM, the next set of four additions in increments of 10 μM and the last set of five additions in increments of 100 μM. Inset in Fig. 6a shows the calibration curve. The sensor exhibits linearity in the range of 1 μM–5 mM with a linear regression equation $i_p(\mu A) = 0.02686 + 0.00416\ C(\mu M)$ $(r = 0.9996)$ and excellent sensitivity of 63.912 μA mM^{-1} cm^{-2}. The detection limit was found to be 0.1 μM. It is worth mentioning that the observed sensitivity in this study was remarkably higher than that of similar AA sensors reported [63, 64].

The stability of the response at higher concentration and fouling due to the oxidized products during the repeated measurements were studied amperometrically by adding higher concentration (100 μM) of AA solution to the constantly stirred PBS solution at 0.2 V. The current response obtained for all additions remains the same and is given by the calibration curve (Fig. 6b). This clearly eliminates the possibility of fouling caused by the oxidized products of AA at the AuNP/PPy/TiO_2.

3.5 Reproducibility and storage stability

The reproducibility of the sensor was evaluated by making five numbers of AuNP/PPy/TiO_2 electrodes and testing with 100 μM AA solution in 0.1 M PBS at 0.2 V. The variation was observed to be <1.5 % (Fig. S5A in the supporting information), which suggests that the electrode modification method adopted in this study was highly reproducible. The sensor was preserved in 0.1 M PBS at room temperature (25 ± 2 °C) when not in use. The long term storage stability of the sensor was examined by measuring the amperometric response to 100 μM AA once in every 3 days over a period of 1 month (Fig. S5B in the supporting information). The decrease in sensitivity was <3 % of its original value. This study has convincingly proved that the sensor has good reproducibility and storage stability.

3.6 Effect of interfering species

The interference of species such as UA, DA, AP and glucose in the determination of AA was studied by amperometric method. Interfering species were injected along with AA into a constantly stirred solution of PBS and their response was noted and presented in Table 1. AA was found to respond in the same way irrespective of the presence or absence of interferences, thus illustrating that the quantitative determination of AA was in no way affected by interfering species. Further, the response current obtained for these interfering species was <7 % of that observed for AA.

Table 1 Steady state current response of AA and other interfering species in PBS solution at 0.2 V

Compounds	Concentration (μM)	Responsecurrent (%)
AA	10	100.00
UA	10	3.23
DA	10	6.51
AP	10	1.54
Glucose	5000	1.96

3.7 Analytical applications

The sensor developed was directly tested for determination of AA in lemon. Fresh juice was injected to 10 ml of constantly stirred solution of 0.1 M PBS and the amperometric response was recorded at 0.2 V and the results are presented in Fig. 7. First three additions are 10 μl and the fourth addition is 100 μl of lemon juice. The concentration of AA was calculated and found to be 339 μg ml^{-1}, which is very close to the value determined by capillary zone electrophoresis [65].

Highly sensitive and selective determination of the AA has been achieved by developing a sensor based on a composite of AuNPs and PPy on TiO_2 nanotube arrays. The oxidation potential of AA at this electrode was very low (0.15 V). The sensor showed linearity over 1 μM–5 mM concentration. The linearity even at very high concentration establishes that no fouling has taken place due to the oxidized products of AA. The interference of other biomolecules was tested and found that the commonly

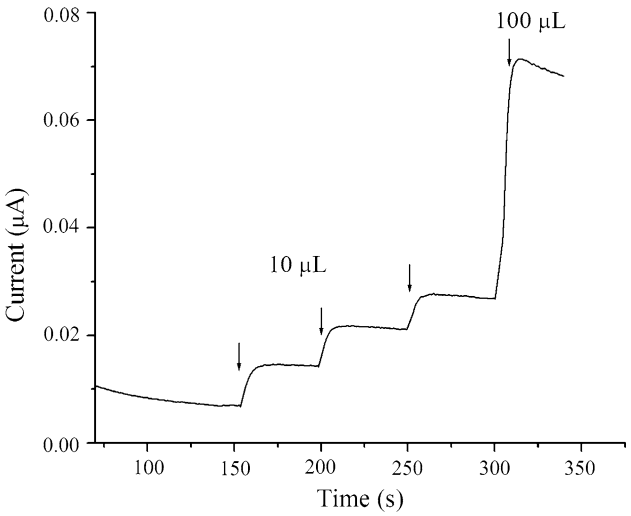

Fig. 7 Steady state current response at 0.2 V on the AuNP/PPy/TiO_2 electrode to lemon juice in a constantly stirred solution of 0.1 M PBS

interfering species did not affect the detection of AA at this electrode. The applicability of this sensor was extended for the testing of AA in lemon.

Acknowledgments T.G.S. thank Prof. A.K. Balakrishnan Nair, Chairman (Admissions), Amrita Vishwa Vidyapeetham for his fruitful suggestions and comments and Dr. A. Ajayaghosh, Scientist H, Photosciences and Photonics division, National Institute for Interdisciplinary Science and Technology, Trivandrum, for AFM analysis.

References

1. Paulose M, Shankar K, Varghese OK, Mor GK, Grimes CA (2006) J Phys D 39:2498
2. Mor GK, Varghese OK, Paulose M, Grimes CA (2003) Sens Lett 1:42
3. Varghese OK, Gong D, Paulose M, Ong KG, Grimes CA (2003) Sens Actuators B 93:338
4. Mor GK, Carvalho MA, Varghese OK, Paulose M, Pishko MV, Grimes CA (2004) J Mater Res 19:628
5. Varghese OK, Mor GK, Grimes CA, Paulose M, Mukherjee N (2004) J Nanosci Nanotechnol 4:733
6. Paulose M, Shankar K, Varghese OK, Mor GK, Hardin B, Grimes CA (2006) Nanotechnology 17:1446
7. Varghese OK, Yang X, Kendig J, Paulose M, Zeng K, Palmer C, Ong KG, Grimes CA (2006) Sens Lett 4:120
8. Yoriya S, Prakasam HE, Varghese OK, Shankar K, Paulose M, Mor GK, Latempa TJ, Grimes CA (2006) Sens Lett 4:334
9. Grimes CA, Ong KG, Varghese OK, Yang X, Mor GK, Paulose M, Dickey, Ruan C, Pishko MV, Kendig JW, Mason AJ (2003) Sensors 3:69
10. Mor GK, Shankar K, Paulose M, Varghese OK, Grimes CA (2006) Nano Lett 6:215
11. Paulose M, Shankar K, Yoriya S, Prakasam HE, Varghese OK, Mor GK, Latempa TA, Fitzgerald A, Grimes CA (2006) J Phys Chem B 110:16179
12. Mor GK, Varghese OK, Paulose M, Shankar K, Grimes CA (2006) Sol Energy Mater Sol Cells 90:2011
13. Paulose M, Varghese OK, Mor GK, Grimes CA, Ong KG (2006) Nanotechnology 17:398
14. Zhu K, Neale NR, Miedaner A, Frank AJ (2006) Nano Lett 7:69
15. Shankar K, Mor GK, Prakasam HE, Yoriya S, Paulose M, Varghese OK, Grimes CA (2007) Nanotechnology 18:11
16. Kafi AKM, Wu G, Chen A (2008) Biosens Bioelectron 24:566
17. Pang X, He D, Luo S, Cai Q (2009) Sens Actuators B 137:134
18. Benvenuto P, Kafi AKM, Chen A (2009) J Electroanal Chem 627:76
19. Han X, Zhu Y, Yang X, Li C (2010) J Alloys Compd 500:247
20. Grimes CA (2007) J Mater Chem 17:1451
21. Cai WY, Xu Q, Zhao XN, Zhu JH, Chen HY (2006) Chem Mater 18:279
22. Daniel MC, Astruc D (2004) Chem Rev 104:293
23. Raj CR, Jena BK (2005) Chem Commun 15:2005
24. Yu AM, Liang ZJ, Cho JH, Caruso F (2003) Nano Lett 3:1203
25. Zhang JD, Oyama M (2005) J Electroanal Chem 577:273
26. Majid E, Hrapovic S, Liu YL, Male KB, Luong JHT (2006) Anal Chem 78:762
27. Templeton AC, Wuelfing WP, Murray RW (2000) Acc Chem Res 33:27
28. El-Deab MS, Ohsaka T (2002) Electrochem Commun 4:288
29. Grabar KC, Freeman RG, Hommer MB, Natan MJ (1995) Anal Chem 67:735
30. Bethell D, Brust M, Schiffrin DJ, Kiely J (1996) J Electroanal Chem 409:137
31. Sagara T, Kato N, Nakashima N (2002) J Phys Chem B 106:1205
32. Kannan P, John SA (2009) Anal Biochem 386:65
33. Ragupathy D, Gopalan AI, Lee KP (2010) Sens Actuators B 143:696
34. Baker SE, Tse KY, Lee CS, Hamers RJ (2006) Diamond Relat Mater 15:433
35. Niedziolka J, Murphy MA, Marken F, Opallo M (2006) Electrochim Acta 51:5897
36. Wang SF, Xu Q (2007) Bioelectrochemistry 70:296
37. Ly SY (2006) Bioelectrochemistry 68:227
38. Wu KB, Wang H, Chen F, Hu SS (2006) Bioelectrochemistry 68:144
39. Zhao G, Xu JJ, Chen HY (2006) Anal Biochem 350:145
40. Jänes A, Kurig H, Lust E (2007) Carbon 45:1226
41. Shankar K, Mor GK, Prakasam HE, Yoriya S, Paulose M, Varghese OK, Grimes CA (2007) Nanotechnology 18:65707
42. Yang LX, He DM, Cai QY (2007) J Phys Chem C 111:8214
43. Roy SC, Paulose M, Grimes CA (2007) Biomaterials 28:4667
44. Popat KC, Eltgroth M, LaTempa TJ, Grimes CA, Desai TA (2007) Biomaterials 28:4880
45. Liu SQ, Chen AC (2005) Langmuir 21:8409
46. Xie Y, Zhou L, Huang H (2007) Biosens Bioelectron 22:2812
47. Kang Q, Yang L, Cai Q (2008) Bioelectrochemistry 74:62
48. Wang C, Yin L, Zhang L, Gao R (2010) J Phys Chem C 114:4408
49. Babu TGS, Suneesh PV, Ramachandran T, Nair B (2010) Anal Lett 43:2809
50. Malinauskas A (1999) Synth Met 107:75
51. Bidan G (1992) Sens Actuators B 6:45
52. Uang YM, Chon TC (2002) Electroanalysis 14:1564
53. Li J, Lin XQ (2007) Anal Chim Acta 596:222
54. Qu L, Xia S, Bian C, Sun J, Han J (2009) Biosens Bioelectron 24:3419
55. Gong J, Wang L, Zhang L (2009) Biosens Bioelectron 24:2285
56. de Tacconi NR, Chenthamarakshan CR, Yogeeswaran G, Watcharenwong A, de Zoysa RS, Basit NA, Rajeshwar K (2006) J Phys Chem B 110:25347
57. Musick MD, Pena DJ, Botsko SL, McEvoy TM, Richardson JN, Natan MJ (1999) Langmuir 15:844
58. Abdelrahman AI, Mohammad AM, Okajima T, Ohsaka T (2006) J Phys Chem B 110:2798
59. Kalimuthu P, John SA (2008) J Electroanal Chem 617:164
60. Raj CR, Tokuda K, Ohsaka T (2001) Bioelectrochemistry 53:183
61. Sivanesan A, Kannan P, John SA (2007) Electrochim Acta 52:8118
62. Li J, Lin X (2007) Sens Actuators B 124:486
63. Foster K, Allen A, Mc Cormac T (2004) J Electroanal Chem 573:203
64. Ambrosi A, Morrin A, Smyth MR, Killard AJ (2008) Anal Chim Acta 609:37
65. Liao T, Jiang CM, Wu MC, Hwang JY, Chang HM (2001) Electrophoresis 22:1484